A bacterial dynamin-like protein
Supplementary Figures and Legends

Supplementary Figure 1

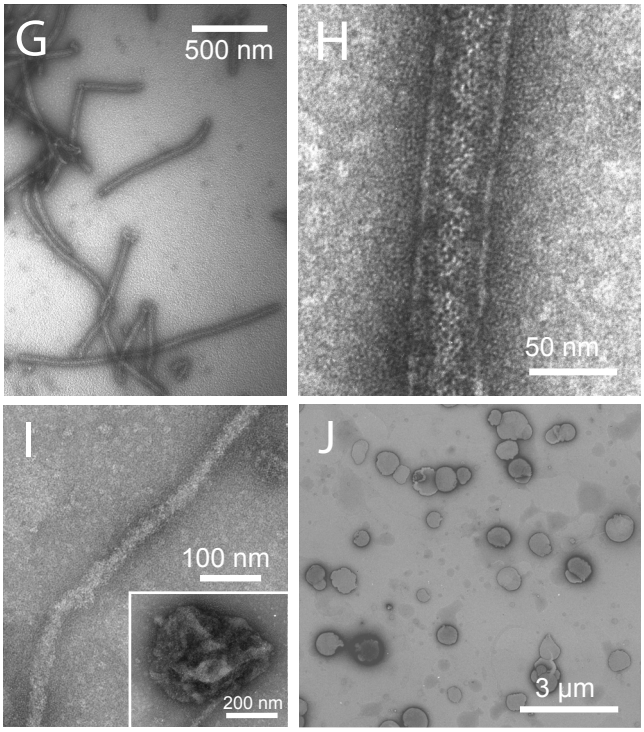

Bacterial dynamin-like protein (BDLP) from *Nostoc* is capable of decorating and tubulating liposomes in different nucleotide states. G-H, In the presence of 2 mM GMPPNP, BDLP (25 *µ*M) decorates and tubulates *E.coli* lipid liposomes. I, In the presence of 1 mM GDP, BDLP (25 *µ*M) also decorates and tubulates *E.coli* lipid liposomes. However, tubes are coated unevenly with a non-regular filamentous array and have variable diameter. Liposomes are often not wholly tubulated (inset). J, *E.coli* whole cell lipid extract extruded to form liposomes.

It should be noted that addition of GTP to BDLP in the presence of *E.coli* lipid liposomes yields decorated tubes that are coated with a mixture of ordered helical polymer similar to that observed in fig. 1D and Supplementary fig. 1G-H, and uneven non-regular filamentous arrays as observed in Supplementary fig. 1I above. Ordered areas of tube are likely due to BDLP associated with GTP whilst less ordered regions reflect nucleotide hydrolysis and a BDLP-GDP coating. 25 *µ*M BDLP in the presence of *E.coli* lipid liposomes but absence of nucleotide forms a disordered coating upon liposomes. Short filamentous arrays may be observed on the liposome surface and sometimes short uneven tubes form. BDLP in the presence of 2 mM GMPPNP alone does not form filaments or rings, and instead seems to form spherical clumps of oligomer.

Supplementary Figure 2

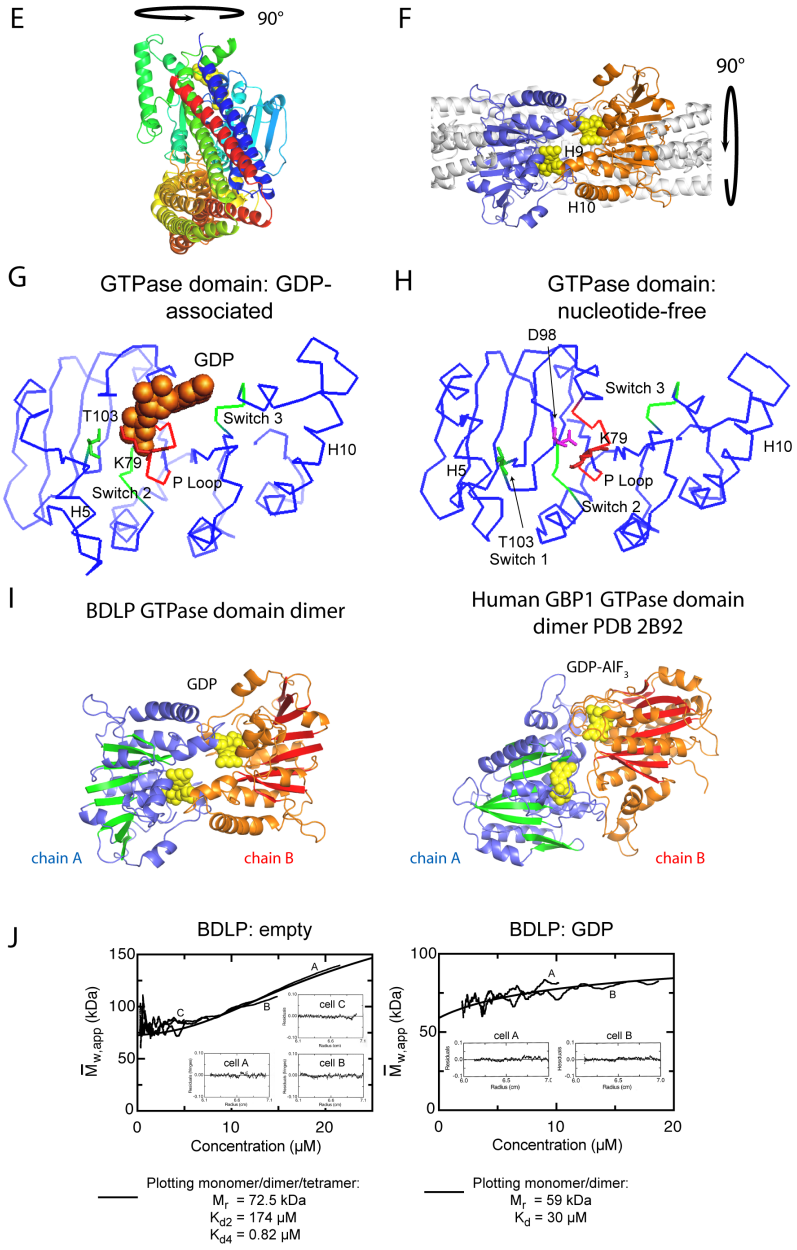

The crystal structure of BDLP in GDP-associated and nucleotide-free conformation. E, Rainbow coloured view of the BDLP-GDP monomer rotated 90˚ to fig. 2A (blue N-terminus through to red C-terminus). F, BDLP-GDP dimer rotated 90˚ to fig. 2B. Glu245 at the C-terminus of helix 9 is in a position to stabilise the nucleotide base bound on the opposing GTPase domain. G-H, Focus on the BDLP GTPase domain mainchain showing residues relevent to the maintext. G, In the presence of GDP, most of the Switch 2 region, including Asp98, is disordered. Lys79 is potentially positioned to modulate catalysis. H, In the absence of nucleotide, Asp98 occludes the active site and Thr103 is angled away from the P-loop. I, Structurally aligned GTPase domain dimers of *N.punctiforme* BDLP and human guanylate-binding protein 1 (PDB entry 2B92). The B chains (orange and red) were superimposed using SSM[29] with 119 aligned Cα atoms, RMSD 2.6 Å and sequence identity 13 %. The figure shows the B chains in both proteins oriented the same way after structural alignment, highlighting essentially the same dimer architecture. The nucleotides are sandwiched between both subunits, but the catalytic centres are only surrounded by residues from a single chain in both structures. Although the dimers are very similar, the A chains show a rotation of about 15° after structural alignment of the B chains. J, analytical ultracentrifugation showing BDLP to be a tetramer in the nucleotide-free form and a dimer in the presence of GDP.

Supplementary Figure 3

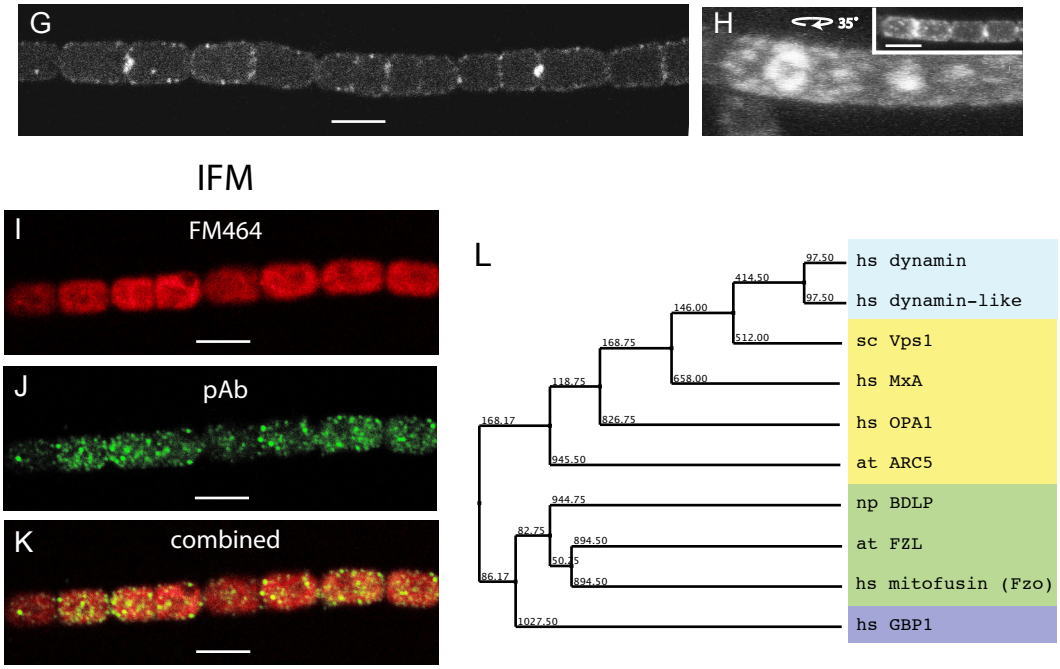

BDLP exhibits a punctate pattern of localisation in filamentous *N.punctiforme*. Scale bars 4 *μ*m. G-H, Rarely, BDLP-GFP preferentially localises to the cell septum. Ring-like architecture can be observed (through confocal 3D reconstruction). I-K, Immunofluorescence microscopy shows punctate localisation predominantly to the cell periphery but also to the interior. L, Evolutionary relationship between dynamin-related proteins. BDLP is most closely related to FZL and Fzo. Database entries for the ten reference sequences used: human dynamin (NP_004399), human dynamin-like protein 1 (NP_036192), yeast Vps1 (NP_012926), human MxA (NP_002453), human OPA1 (O60313), Arabidopsis ARC5 (NP_188606), Nostoc BDLP (ZP_00108538), Arabidopsis FZL (ABE96616), human mitofusin (Fzo, NP_284941), human GBP1 (NP_002044).

Supplementary Methods

Cloning, expression and purification. The coding sequence for ZP_00108538 from *Nostoc punctiforme*, which we term BDLP, was amplified using PCR from genomic DNA obtained from ATCC (#29133D). The gene was cloned into pOPTM vector (a gift from Dr. Olga Perisic, MRC Laboratory of Molecular Biology, Cambridge, UK) which yields a N-terminal MBP fusion with a TEV cleavage site in the linker, and a hexa-histidine tag at the C-terminus. Expression was in *E.coli* BL21(DE3) strain at 22°C overnight. The BDLP-MBP fusion was purified using a nickel-Sepharose strategy. The lysate buffer consisted of 50 mM Tris-Cl, 1.25 M sodium chloride, final pH 8.0, the wash buffer of 50 mM Tris-Cl, 500 mM sodium chloride, 20% glycerol, final pH 8.5, and elution buffer of 50 mM Tris-Cl, 1 M imidazole, final pH 8.5. For seleno-methionine (SeMet) purification all buffers remained the same except for an additional 5 mM DTT, although 1% CHAPS was also required in the lysis buffer. For the general SeMet purification strategy see Supplementary Reference[30]. Imidazole was removed by Sephadex G25 buffer exchange into 50 mM Tris-Cl, 500 mM sodium chloride, 20% glycerol, final pH 8.5. The fusion protein was cleaved by TEV protease and the products separated by Sephacryl S300 gel filtration (Amersham Biosciences, Sweden) equilibrated in 20 mM Tris-Cl, 1 mM EDTA, 1 mM sodium azide, final pH 7.5. Purified BDLP is full length and includes an additional Gly-Ser-His at the N-terminus and 6x His at the C-terminus, as confirmed by electrospray mass spectrometry (79.5 kDa).

Crystallisation, structure determination and refinement. Initial BDLP crystallisation conditions were found from a 1500 condition screen set up using a high-throughput nanolitre robotic system[28]. Native (no nucleotide/empty) and seleno-methionine BDLP was crystallised by sitting drop vapour diffusion against a mother liquor of 100 mM Tris-Cl pH 7.1, 3.5 % polyethylene glycol 6000 (PEG), 100 mM potassium chloride. Artificial mother liquor mixed with 27 % glycerol as cryoprotectant was added directly to the drop before crystals were flash frozen in liquid nitrogen. Native crystals grew in the monoclinic space group C2 with cell dimensions a=214.3 Å, b=218.6 Å, c=151.2 Å, β=134.8°. SeMet BDLP grew in the tetragonal space group I422, a=b=152.0 Å, c=220.3 Å. GDP-associated BDLP required incubation with 2 mM GDP and 3 mM magnesium sulphate at 37°C before crystallisation against a mother liquor of 100 mM sodium acetate pH 4.55, 3.5% PEG 4000, 15 % glycerol. Crystals were briefly immersed in a cryoprotectant consisting of artificial mother liquor mixed with 17 % methyl pentanediol (MPD), 2 mM magnesium sulphate and 2 mM GDP before being flash frozen in liquid nitrogen. Crystals were orthorhombic in space group I222, a=77.6 Å, b=154.9 Å, c=247.9 Å. The *de novo* crystal structure of BDLP in the nucleotide-free form was solved initially using crystals containing a mutant with four isoleucine residues mutated to methionine (I329M, I557M, I567M, I635M) to increase anomalous

signal. A three-wavelength MAD experiment performed on beamline ID14eh4 at ESRF, Grenoble, yielded good phases suitable for building a Cα trace at 4.0 Å resolution (Supplementary Table 1). Phase extension using the higher resolution native dataset and the Cα model enabled completion of the model and refinement to 3.0 Å resolution (Table 1). 90.4 % of residues are in the 'most favored region' of the Ramachandran plot with 0.0 % outliers. Crystals obtained with BDLP in the presence of GDP were solved using molecular replacement (PHASER) with the model of the nucleotide-free form obtained in this study. The model was then rebuilt and refined to 3.1 Å resolution (Table 1). 85.6 % of residues are in the 'most favored region' of the Ramachandran plot with 0.0 % outliers. Coordinates have been deposited in the Protein Data Bank with accession codes 2J69 (BDLP empty) and 2J68 (BDLP GDP).

Electron microscopy and GTPase assays. For the production of liposomes, 5 mg *E.coli* whole cell lipid extract was dissolved in 450 μl chloroform and 50 μl methanol, lyophilised by evaporation with nitrogen gas, desiccated for 1 hr and resuspended in reaction buffer A- 20 mM HEPES, 130 mM sodium chloride, 5 mM potassium chloride, 1 mM EGTA, 2 mM magnesium sulphate, final pH 7.2. After brief sonication with a micro-tip sonicator, liposomes were generated by extrusion through either a 1 μM or 0.2 μM filter. For tubulation, 1 mM nucleotide, either GMPPNP (2 mM), GTP or GDP was incubated at 37°C for 10 min with 25 μM BDLP and 2 mg/ml liposomes. Grids were stained with 2 % uranyl acetate and examined on a Phillips EM208 electron microscope. GTPase assays were performed at room temperature and utilised reaction buffer A. BDLP and GTP concentration was at 2.5 μM and 1 mM, respectively. Free phosphate concentration was determined using a malachite green based kit (Innova Biosciences, UK, #302-0500).

BDLP antibody preparation. Antibody against BDLP was raised in rabbit and affinity purified using BDLP covalently coupled to Sepharose 4B. Affinity purification protocol was as follows: 15 ml of rabbit antiserum was clarified for 10 mins at 3000 rpm and then passed repeatedly over a 2 ml BDLP-Sepharose column at 4˚C. After extensive washing with chilled PBS, elution was with 0.15 M glycine-Cl, final pH 2.5. Eluate was collected in 600 μl fractions and the pH immediately neutralised with basic 1 M Tris to a final pH= ~7.5. 10 % glycerol was added to fractions for storage at -20˚C.

Western blot. Blotted PVDF membrane was blocked for 1 hr in phosphate buffered solution/Tween (PBST) supplemented with 5 % milk powder. 1:1,300 primary BDLP antibody was directly added and incubated for 1 hr. After washing 1:4,000 HRP-goat anti-rabbit IgG secondary antibody (AbCam, UK) was added for 1 hr. Visualisation was with the ECL Western Blotting Detection Reagents (Amersham) and autoradiographic film.

Immunofluorescence microscopy (IFM). For IFM, cells were fixed in 4 % paraformaldehyde and treated with lysozyme at 10 mg/ml. 1:50 primary BDLP antibody

and 1:100 secondary anti-rabbit-FITC concentration was utilised. SlowFade antifade (Molecular Probes, USA) and membrane stain FM 4-64 was added. Images were collected on a Nikon LHS-H100P-1 microscope and Biorad Radiance 2000 scanning system (confocal).

Construction of BDLP-GFP reporter. The BDLP coding sequence plus 700 base pairs upstream of the translational start was cloned into pSCR202, a *Nostoc p*. shuttle vector[31], with a *gfp* translational fusion at the C-terminus. This was transformed into wild type *Nostoc p*. and transformants selected with 10 μg/ml ampicillin in liquid media.

Phylogenetic analysis. Only the GTPase domains of dynamin-related proteins are suitable for sequence analysis since the middle domains largely consist of helical bundles (related to coiled-coil structures) that dominate the sequences. For the phylogenetic tree, 10-20 sequences related to the different classes of dynamin-related proteins were picked from the database and aligned against each other in groups. The GTPase domains were then cut out and combined into a larger alignment and re-aligned using CLUSTALW and a tree-calculated (UPGMA, unweighted pair-group method using arithmetic averages, similarity calculated using BLOSUM62 scores). Database entries for the reference sequences used are listed in the figure legend (see Supplementary fig. 3L).

Supplementary References

29. Krissinel, E. & Henrick, K. Secondary-structure matching (SSM), a new tool for fast protein structure alignment in three dimensions. Acta Crystallogr D 60, 2256-68 (2004).

30. Van Duyne, G. D., Standaert, R. F., Karplus, P. A., Schreiber, S. L. & Clardy, J. Atomic structures of the human immunophilin FKBP-12 complexes with FK506 and rapamycin. J Mol Biol 229, 105-24 (1993).

31. Summers, M. L., Wallis, J. G., Campbell, E. L. & Meeks, J. C. Genetic evidence of a major role for glucose-6-phosphate dehydrogenase in nitrogen fixation and dark growth of the cyanobacterium *Nostoc sp*. strain ATCC 29133. J Bacteriol 177, 6184-94 (1995).

Supplementary Table 1

Crystallographic data

***Nostoc punctiforme* bynamin (ZP_00108538, GSH-1-693-HHHHHH)**

Crystal	λ[Å]	resol.	I/σI[1]	Rm[2][%]	m	ultipl.[3]	Compl.[%][4]
bynamin MAD (mutant I329M, I557M, I567M, I635M) SeMet, I422, a=b=152.0 Å, c=220.3 Å							
PEAK	0 .9789	4.0 Å	19.9(9.8)	0 .127(0.273)		14.1(7.6)	99.8(99.8)
INFL	0 .9797	4.0 Å	19.2(9.4)	0 .128(0.279)		14.1(7.6)	99.8(99.8)
REM	0.9763	4.0 Å	18.5(8.4)	0 .139(0.325)		14.1(7.7)	99.8(99.8)
bynamin empty, C2, a=214.3 Å, b=218.6 Å, c=151.2 Å, β=134.8°							
EMPTY	0.9795	3.0 Å	1 0.3(1.8)	0.059(0.397)		1.9	98.6(98.5)
bynamin GDP, I222, a=77.6 Å, b=154.9 Å, c=247.9 Å							
GDP	0.9763	3.1 Å	15.6(3.3)	0 .070(0.328)		3.5	99.6(99.6)

[1]signal to noise ratio for merged intensities (highest resolution bins in brackets). [2]Rm: $\Sigma h \Sigma i |I(h,i)-I(h)| / \Sigma h \Sigma i\ I(h,i)$ where I(h,i) are symmetry related intensities and I(h) is the mean intensity of the reflection with unique index h. [3]Multiplicity for unique reflections, anomalous multiplicity in brackets. [4]Completeness for unique reflections, anomalous completeness in brackets. The correlation coefficient between anomalous differences (PEAK, REM) was 0.39.